Internal gravity wave emission from a pancake vortex: An example of wave–vortex interaction in strongly stratified flows

R. Plougonven[a] and V. Zeitlin
Laboratoire de Météorologie Dynamique, Ecole Normale Supérieure, 24 rue Lhomond, 75231 Paris Cedex 05, France

(Received 13 March 2001; accepted 12 December 2001)

At small Froude numbers the motion of a stably stratified fluid consists of a quasisteady vortical component and a propagating wave component. The vortical component is organized into layers of horizontal motions with well-pronounced vertical vorticity and often takes the form of so-called ''pancake'' vortices. An analytical model of such a vortex that is a solution of the Euler–Boussinesq equations at a vanishing Froude number is constructed as a superposition of horizontal two-dimensional Kirchhoff elliptic vortices. This vortex is nonstationary and internal gravity waves are, therefore, excited by its motion. The radiation properties are studied by matching the vortex field with the far internal gravity wave field according to the procedure applied in acoustics to determine vortex sound. The structure of the gravity wave field is completely quantified. By calculating energy and angular momentum fluxes carried by outgoing waves and attributing them to the adiabatic change of the vortex parameters, we calculate the backreaction of the internal gravity waves radiation and show that, as in the case of acoustic radiation by the Kirchhoff vortex, this adiabatic evolution leads to an elongation of the vortex, and its eventual destabilization. © *2002 American Institute of Physics.* [DOI: 10.1063/1.1448297]

I. INTRODUCTION

As was shown in the pioneering papers[1,2] (for a recent review, see Ref. 3), strongly stratified flows are split, in the leading order in the Froude number, which is defined as a ratio of buoyancy to advection time scales, into mutually noninteracting vortex and wave components. The former is concentrated in horizontal layers with a well-pronounced vertical vorticity and, as stratification inhibits vertical motion, follows the two-dimensional (2-D) incompressible Euler dynamics[1–3] at the leading order.

The horizontal layering in strongly stratified flows has been confirmed in a number of analytic, numerical, and experimental studies. Moreover, numerical simulations in Ref. 4 and later works have shown that coherent discus-shaped ''pancake'' vortices tend to emerge from an initially random field of decaying turbulence in a stratified fluid. Such vortices are also recurrent in laboratory studies of wakes in a stratified fluid: in the wake of a towed sphere,[5,6] or in decaying turbulence behind a towed grid.[7,8] Layering structure and the ensuing vortices have also been observed during the late stages of instability of tall columnar vortices in the stratified fluid.[9–11] A rather detailed study of the internal structure of the pancake vortices was undertaken experimentally in Refs. 12 and 6 and numerically in Ref. 13. It was found that these vortices obey the cyclostrophic balance conditions and exhibit a pinching of the isopycnals near the core. Pancake vortices are, thus, a universal feature of stratified flows.

The other component of the flow, the internal gravity waves (IGW), is thoroughly studied (e.g., Ref. 14), especially in the linear context. Emission of IGW by the above-mentioned wakes is well documented[15,16] and the splitting of IGW from the vortex component is well seen, for example, while studying analytically the initial-value problem for small disturbances discussed in Ref. 17: a small initial perturbation in a stratified fluid splits into a outward propagating IGW packet and a residual steady vortex (vortical motion here is steady only because of the linearization of the equations, in the next approximation its slow evolution appears—cf. Ref. 18). The vertical vorticity plays a crucial role in such an analysis as it allows one to determine the whole of the vortical flow by inversion. The vertical vorticity is the leading-order residue of Ertel's potential vorticity (PV): $q = \nabla\rho\cdot\boldsymbol{\omega}$, where ρ is density and $\boldsymbol{\omega}$ is the total vorticity. One can reconstruct the whole slow vortical field in higher orders as well using subsequent approximations for the PV, if only the splitting persists and the fastly outgoing wave component can still be consistently filtered out. Thus, the problem of the persistence of splitting in the higher approximations is equivalent to the problem of the slow manifold (cf., e.g., Ref. 19) in strongly stratified fluid dynamics, i.e., a subspace in the whole phase space of the system such that, once projected on it, the dynamics stays there and may be traced for long times without taking care of the fast wave motions. The possibility to filter out waves is practically very important (weather forecasting is, probably, the best example) and much understanding of atmosphere and ocean dynamics has come from the no-wave ''balanced'' models. It is also important in any kind of numerical simulations in stratified turbulence as (at least some part of) the wave activity is usually considered as a subgrid one. Therefore, a study of the

[a]Author to whom correspondence should be addressed. Telephone: (33) 1 44 32 22 21; fax: (33) 1 43 36 83 92; electronic mail: riwal.plougonven@polytechnique.org

vortex–wave interaction mechanisms is crucial in this context as it allows us to check the validity of splitting and slow-manifold ideas and to establish their limitations.

One of the essential mechanisms of wave–vortex interactions is well documented in acoustics: it is the emission of sound waves by vortices (vortex sound). As was shown in the pioneering paper by Lighthill,[20] nonstationary vortex motions act as sources of sound waves in a compressible fluid. The theory of this phenomenon was developed for small Mach numbers when the vortex size is much smaller than the characteristic sound-wave length. Pressure fluctuations of the *incompressible* fluid produced by the unsteady vortex in its vicinity may be related to the pressure fluctuations in the *compressible* far wave field, by comparing corresponding asymptotics. Mathematically, the rigorous basis for this description was established in the work of Crow,[21] where the theory of matched asymptotic expansions in the inner (vortex) and outer (wave) regions were used. It was shown that the problem is well posed for small Mach numbers. The idea of vortex sound has been subsequently used to determine acoustic radiation from numerous vortex flows (e.g., Refs. 22, 23).

A step further in the vortex sound theory was made when it was realized that the backreaction of the radiation can be calculated by attributing energy and angular momentum losses due to the sound-wave emission to a slow adiabatic evolution of the vortex parameters. This has been done for the first time in the axisymmetric case of two coaxial ''leapfrogging'' vortex rings;[24] in planar situations, various configurations of point vortices were investigated along these lines in Ref. 25, where radiation-induced vortex collapse was discovered. Finally, in Ref. 26, a distributed vortex structure—the Kirchhoff vortex (an elliptic patch of uniform vorticity surrounded by irrotational fluid cf., e.g., Ref. 27) was studied. Using matched asymptotic expansions, as in Ref. 21, the sound waves emitted by the vortex were calculated. Assuming that the parameters of the vortex varied slowly in response to the loss of energy and angular momentum due to the waves in the adiabatic approximation, the Kirchhoff vortex was found to elongate on a time scale $M^{-4}T_0$, where $M=U/c$ is the Mach number (U is the characteristic vortex velocity and c is the velocity of sound) and $T_0=U/L$ is the advective time scale (L is the characteristic vortex scale), the same time scale as for a pair of point vortices of equal sign found in Ref. 25.

The shallow water equations being equivalent to a 2-D compressible fluid with a specific equation of state, the same ideas were later used for an elliptic Kirchhoff vortex in the rotating shallow water (RSW) equations,[28] with special attention paid to the effect of rotation. In the SW or RSW context, the waves in question are gravity waves, and the Froude number $F=U/\sqrt{gH}$ replaces the Mach number. The waves were found to be radiated at $\mathcal{O}(F^2)$. They are responsible for a flux of energy and angular momentum away from the vortex at $\mathcal{O}(F^4)$, and induce a slow evolution of the vortex on a time scale $T_2=F^{-4}T_0$, where T_0 is the vortex advection time scale. The method used was a direct multitime scale perturbation expansion within the framework of the conformal dynamics for 2-D vortex patches that was proposed in Ref. 29 and allows a calculation of eventual departures from the elliptic shape of the vortex in the course of its slow evolution. It was shown that the presence of rotation results in the appearance of logarithmic terms $\mathcal{O}(F^n \log F)$ in the asymptotic expansion. Using symbolic computer computations, the analysis was performed up to terms $\mathcal{O}(F^2 \log F)$ under a simplifying reflectional symmetry assumption and was stopped at $\mathcal{O}(F^4)$, as it was impossible to obtain closed analytic expressions for higher-order corrections.

The phenomenon of Lighthill radiation is conceptually important in the context of geophysical fluid dynamics because it invalidates the idea of a strict slow manifold mentioned above: even a purely vortical initial condition (i.e., one exactly projected onto the would-be slow manifold) will, if unsteady, radiate gravity waves and be altered at long times by the backreaction of this radiation. Past a certain time, a wave-filtered description of the flow becomes, thus, erroneous. In the RSW context, the limitations imposed on the concepts of balance, slow manifold, and potential vorticity inversion by the Lighthill radiation were recently discussed in detail in Ref. 19.

In the present paper, by applying the vortex sound philosophy to the vortex motions in a stably stratified fluid, we make a step forward in studying wave emission by vortices and their backreaction by departing both from the two-dimensionality of the previous studies and the isotropy of sound waves (or surface inertia-gravity waves in the RSW context). The wave emission from a localized nonstationary region of uniform potential vorticity is calculated within the framework of the Euler equations in the Boussinesq approximation (Euler–Boussinesq in what follows) for a stratified fluid with a constant background stratification (constant Brunt–Väisälä frequency). The Boussinesq approximation means that sound waves are filtered out and only internal gravity waves (IGW) may propagate in the medium. For simplicity we will consider a nonrotating fluid below.

In order to carry out the calculations explicitly, we construct a simple unsteady pancake vortex, which we call a 3-D Kirchhoff vortex: a region of uniform potential vorticity with elliptic horizontal cross sections. All the horizontal ellipses bounding the vortex have the same aspect ratio and rotate at the same angular frequency. Vortices of this kind have been studied (Refs. 30 and 31) in the context of the quasigeostrophic equations. As to our knowledge, this configuration was not considered in the case of the Euler–Boussinesq equations. We will suppose in the following, as is often the case in the observed strongly stratified flows, that the height of the vortex is much smaller than its horizontal length scale: $L \gg H$.

The paper is organized as follows: in Sec. II, the 3-D Kirchhoff vortex is constructed using conformal dynamics in each horizontal plane.[29,28] The scaling for the farfield, the matching of the far asymptotics of the latter is done in Sec. III. Finally, the backreaction on the vortex is calculated in Sec. IV. Section V contains a summary and a discussion.

II. THREE-DIMENSIONAL KIRCHHOFF VORTEX IN A STRONGLY STRATIFIED FLUID

We first recall the Euler–Boussinesq (EB) equations for a stratified fluid in the form we use below:

$$D_t \mathbf{u}_H + \rho_0^{-1} \nabla_H P = 0, \tag{1a}$$

$$D_t w + \rho_0^{-1} \partial_z P - \xi = 0, \tag{1b}$$

$$\nabla_H \cdot \mathbf{u}_H + \partial_z w = 0, \tag{1c}$$

$$D_t \xi + N^2 w = 0, \tag{1d}$$

where $\mathbf{u}_H$ is the horizontal and w is the vertical velocity, respectively ($\mathbf{u}$ will denote the full 3-D velocity below), ξ is buoyancy ($\xi = -\rho g/\rho_0$, where ρ is the density perturbation and ρ_0 is the basic state density), N is the Brunt–Väisälä frequency and $D_t = \partial/\partial t + u\partial/\partial x + v\partial/\partial y + w\partial/\partial z$ is the advective derivative. Note that these equations are not hydrostatic. Yet the scaling we use corresponds to hydrostaticity at the leading order.

A. Preliminary scaling considerations

The solution of the wave emission problem by an unsteady vortex by means of the method of matched asymptotic expansions is well posed,[21] provided there is a scale separation between the length scale of the waves and that of the vortex. Here we find constraints imposed by this requirement on a vortex of characteristic horizontal scale L and characteristic height H.

If U is the characteristic horizontal velocity in the vortex region the advective time scale is $T = L/U$. We suppose that this time scale is much greater than the buoyancy period: $F_H = U/NL \ll 1$. As the ultimate mechanism of IGW excitation are the pressure fluctuations due to unsteadiness of the vortex flow, they are expected to have the same vertical length scale as these latter, i.e., H, and the same time scale. The dispersion relation for low-frequency IGW: $\Omega^2 = N^2 k_H^2/k_\perp^2$, where Ω is wave frequency and k_H, $k_\perp$ are horizontal and vertical wave numbers, respectively, yields $U/L \sim NH/\lambda$. This gives an expression of the characteristic wavelength λ in terms of L:

$$\lambda = \frac{NH}{U} L = \frac{1}{F} L, \quad \text{with } F = \frac{U}{NH}. \tag{2}$$

Hence, for wave-vortex scale separation we need to have

$$F = \frac{U}{NH} \ll 1. \tag{3}$$

Here F will be the small parameter used in the asymptotic expansions below.

B. Scaling in the inner (vortex) region

In the vicinity of the vortex the motion is essentially horizontal. To make the separation between the vortex and wave motions clear, we can rewrite Eqs. (1a)–(1d) using the Helmholtz decomposition for the horizontal velocity:

$$\mathbf{u} = +\mathbf{e}_z \times \nabla_H \psi + \nabla_H \phi + w \mathbf{e}_z. \tag{4}$$

Instead of Eqs. (1a)–(1d), the divergence of (1a)+(1b) and the horizontal curl of (1a) will be used below.

The scaling is the same as in Ref. 3 (and references therein), with some minor differences. The horizontal and vertical coordinates $\mathbf{x}$, z are scaled as L and H, respectively; $\mathbf{u}_H$ has a scale U, and t scales as U/L. By virtue of the continuity equation, w scales as UH/L. In the buoyancy equation, the ratio of $D_t \xi$ over $N^2 w$ scales as $F^2 = (U/NH)^2$, the square of the vertical Froude number. Finally, in order to keep only one parameter, we assume that F and the aspect ratio H/L are comparable. The nondimensionalized EB equations are

$$\partial_z(\partial_z P - \xi) + F^2[\Delta_H P + \nabla \cdot (\mathbf{u} \cdot \nabla \mathbf{u})] = 0, \tag{5a}$$

$$\partial_z P - \xi + F^2(\partial_t w + \mathbf{u} \cdot \nabla w) = 0, \tag{5b}$$

$$w + F^2(\partial_t \xi + \mathbf{u} \cdot \nabla \xi) = 0, \tag{5c}$$

$$\partial_t \Delta_H \psi + \mathcal{J}(\psi, \Delta_H \psi) + \nabla_H \cdot (\nabla_H \phi \Delta_H \psi) + w \partial_z \Delta_H \psi + \nabla w \nabla \partial_z \psi + \mathcal{J}(w, \partial_z \phi) = 0, \tag{5d}$$

$$\Delta_H \phi + \partial_z w = 0, \tag{5e}$$

where $\mathcal{J}$ denotes the horizontal Jacobian: $J(a,b) = \partial_x a \partial_y b - \partial_x b \partial_y a$.

Using the above scaling we get for PV:

$$q = \omega \cdot \nabla \theta = \Delta_H \psi + F^2[\xi_z \Delta_H \psi - \xi_x \psi_{zx} - \xi_y \psi_{zy} + \mathcal{J}(\phi_z, \xi)] + F^4 \mathcal{J}(\xi, w). \tag{6}$$

All variables are expanded in an asymptotic series in F^2:

$$\psi = \psi_0 + F^2 \psi_1 + F^4 \psi_2 + \mathcal{O}(F^6). \tag{7}$$

At zeroth order in F^2, Eq. (5c) yields $w_0 = 0$. Through (5e), ϕ_0 is also zero, and we get

$$w_0 = 0, \tag{8a}$$

$$\phi_0 = 0, \tag{8b}$$

$$\partial_t \Delta_H \psi_0 + J(\psi_0, \Delta_H \psi_0) = 0, \tag{8c}$$

$$\Delta_H P_0 = -\nabla \cdot (\mathbf{u}_0 \cdot \nabla \mathbf{u}_0), \tag{8d}$$

$$\xi_0 = \partial_z P_0, \tag{8e}$$

where $\mathbf{u}_0 = +\mathbf{e}_z \times \nabla_H \psi_0$.

The motion at the leading order is, therefore, purely horizontal and vortical (bidimensionalization). Equation (8c) is equivalent to the 2-D Euler equations for incompressible fluid, where z enters as a parameter. Hence, within this accuracy it is possible to build a three-dimensional vortex as a stack of 2-D Euler ones. The vertical profile should be chosen carefully in order not to invalidate the coherence of motions in different horizontal planes and to avoid unphysical vertical gradients. Once ψ_0 is obtained from the PV distribution, the rest of the zeroth-order fields and higher-order corrections can be determined from ψ_0: for example, (8d) determines pressure and (8e) determines buoyancy; w_1 will then be determined from ψ_0 and ξ_0 through (5c).

C. Construction of the 3-D Kirchhoff vortex

A 3-D vortex in a stratified fluid is built from the same principle as in shallow water:[28] a bounded region of fluid having homogeneous PV (equal to unity) is taken; it is surrounded by fluid with zero PV where the flow follows from the PV inversion. The 3-D region of homogeneous PV is defined as follows: the intersection of each horizontal plane with the region of nonzero PV is an ellipse; all such ellipses are centered at the same vertical axis and have the same aspect ratio and orientation. Hence, the vortex region is entirely defined by (1) the aspect ratio, (2) the orientation, and (3) the vertical profile $\gamma(z)$ of the length of the major axis in each horizontal plane.

The flow in every horizontal plane (for every z) will be calculated using the conformal dynamics approach,[29] which uses conformal mappings to parametrize the patches of uniform vorticity on the plane. In each horizontal plane, an interior and an exterior region will be considered; the flow in the latter is described via a mapping of the exterior of the unit disk in the auxiliary ζ plane onto the exterior of the ellipse in the physical plane, or χ plane, where $\chi=x+iy$. As the ellipses rotate and as their size varies with z these mappings depend parametrically on z and are time periodic.

The expression for q at order 0 will account for the totality of PV, being equal to unity inside the vortex region and zero outside. All higher-order corrections to q will thus vanish, which allows us to determine perturbatively the hydrodynamical fields in an unambiguous way.

At order 0, as can be seen from (6), PV coincides with the vertical vorticity, $\Delta_H\psi$, entirely determined by the horizontal velocity. Hence the same equations as in the SW case[28] result, with z as a parameter, and we simply state the result.

The mapping of the exterior of the unit disk in the ζ plane onto the exterior of the ellipse in the physical χ plane is given by

$$g(\zeta)=\Gamma(z)\zeta+\frac{\nu(z)e^{i\omega t}}{\zeta}, \tag{9}$$

where g depends on z and t parametrically, and $\Gamma(z)$ and $\nu(z)$ are supposed to be real and positive for all z and such that $\nu(z)<\Gamma(z)$. The major and minor semiaxes of each ellipse are $\Gamma(z)\pm\nu(z)$, respectively. As the aspect ratio of all the ellipses in the stack is the same, Γ and ν have the same vertical profile:

$$\Gamma=\Gamma_0\gamma(z), \quad \nu=\nu_0\gamma(z), \tag{10}$$

where Γ_0 and ν_0 are real and positive.

The rotation frequency ω is determined by the geometrical parameters of the ellipses (and by the value of PV, here unity):

$$\omega=\frac{1}{2}\left(1-\frac{\nu(z)^2}{\Gamma(z)^2}\right). \tag{11}$$

In the interior region $\chi=x+iy$ is the complex space coordinate, and horizontal velocity is

$$v_0^{(i)}(\chi,\overline{\chi},z,t)=\frac{i}{2}\left(\chi-\frac{\nu_0 e^{i\omega t}}{\Gamma_0}\overline{\chi}\right). \tag{12}$$

Note that there is no vertical shear inside the vortex.

In the exterior region, all fields are considered as functions of ζ, $\overline{\zeta}$, z, and t, where ζ and $\overline{\zeta}$ correspond to the location defined by $\chi=x+iy=g(\zeta)$. The velocity is

$$v_0^{(e)}(\zeta,\overline{\zeta},z,t)=\frac{i}{2\Gamma_0}(\Gamma_0^2-\nu_0^2)\gamma(z)\frac{1}{\overline{\zeta}}=i\Gamma_0\omega\gamma(z)\frac{1}{\overline{\zeta}}. \tag{13}$$

The vertical profile $\gamma(z)$ has to be a sufficiently smooth function with compact support (of order one, due to the choice of scaling). In what follows, we choose this profile to be symmetric in z and normalized:

$$\int_{-\infty}^{\infty} ds\,\gamma(s)^2=1. \tag{14}$$

For instance, one can take

$$\begin{aligned}&\gamma(z)=K(z^2-1)^2, \quad \text{for } -1<z<1,\\ &\gamma(z)=0, \quad \text{for } |z|>1,\end{aligned} \tag{15}$$

where K is a normalization constant.

D. Pressure, buoyancy, and vertical velocity fields

The pressure field can be obtained directly by integrating the equation of horizontal motion (1a):

$$\nabla P_0=-\partial_t\mathbf{u}_0-\mathbf{u}_0\cdot\nabla\mathbf{u}_0. \tag{16}$$

The following expressions follow:

$$P_0^{(i)}=\frac{\omega}{4}\left(\chi\overline{\chi}-\frac{1}{2\Gamma_0}(\nu_0 e^{-i\omega t}\chi^2+\nu_0 e^{i\omega t}\overline{\chi}^2)\right)-\omega^2\Gamma_0^2\gamma^2(z), \tag{17a}$$

$$P_0^{(e)}=\frac{\omega^2\Gamma_0^2}{2}\left[-\frac{1}{\zeta\overline{\zeta}}+\frac{1}{2\Gamma_0}\left(\frac{\nu_0 e^{i\omega t}}{\zeta^2}+\frac{\nu_0 e^{-i\omega t}}{\overline{\zeta}^2}\right)\right]\gamma^2(z). \tag{17b}$$

From (8d), the buoyancy field can be obtained:

$$\xi_0^{(i)}=-2\Gamma_0^2\omega^2\gamma(z)\gamma'(z), \tag{18a}$$

$$\xi_0^{(e)}=-\Gamma_0^2\omega^2\left(\frac{\Gamma_0\zeta\overline{\zeta}^{-1}-\nu_0 e^{i\omega t}}{\Gamma_0\zeta^2-\nu_0 e^{i\omega t}}+\text{c.c.}\right)\gamma(z)\gamma'(z). \tag{18b}$$

The vortex is in the cyclostrophic balance by construction. Hence, its core corresponds to a low-pressure anomaly and, as follows from the hydrostatic balance, buoyancy must have a negative anomaly in the lower part of the vortex and a positive anomaly in the upper part. This is exactly the case in (18a), which is illustrated in Fig. 1. Inside the vortex the isopycnals are horizontal and pinch, making the density gradient steeper, like in the observed vortices.[6,13] One should be cautious, however, while comparing our inviscid construction with viscous simulations. For instance, vertical vorticity at the first order has a discontinuous distribution in our ana-

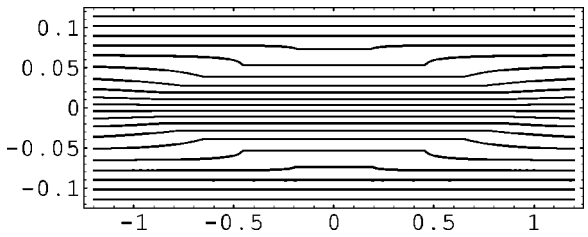

FIG. 1. Isopycnals at leading order in the plane of the minor axis. Note that the isopycnals are horizontal inside the vortex.

lytical model; in laboratory experiments, vortices commonly exhibit vorticity distributions of the Gaussian type.[8]

Vertical velocity and horizontal velocity potential are absent in the leading order; hence, the equations of motion at $\mathcal{O}(F^2)$ are needed to determine them:

$$w_1 = -(\partial_t \xi_0 + \mathbf{u}_0 \cdot \boldsymbol{\nabla}_H \xi_0), \tag{19a}$$

$$\Delta_H \phi_1 = -\partial_z w_1 . \tag{19b}$$

The vertical velocity following from (19a) has a rather complex form because of the time dependence of the mapping (9):

$$w_1^{(i)} = 0, \tag{20a}$$

$$w_1^{(e)} = i\gamma(z)\gamma'(z)\Gamma_0^3\omega^3 \Bigg[\frac{1}{(\Gamma_0\zeta^2 - \nu_0 e^{i\omega t})^2} \times \Bigg(\nu_0 e^{i\omega t}(\zeta\bar{\zeta}^{-1} - \zeta^2) - 2\zeta^2 \frac{(\Gamma_0\zeta\bar{\zeta}^{-1} - \nu_0 e^{i\omega t})^2}{\Gamma_0\zeta^2 - \nu_0 e^{i\omega t}} - \frac{(\nu_0 e^{-i\omega t}\zeta^2 - \nu_0 e^{i\omega t}\bar{\zeta}^2)(\Gamma_0\zeta\bar{\zeta}^{-1} - \nu_0 e^{i\omega t})}{\zeta\bar{\zeta}(\Gamma_0\bar{\zeta}^2 - \nu_0 e^{-i\omega t})} \Bigg) - \text{c.c.} \Bigg]. \tag{20b}$$

The vertical velocity is zero inside the vortex and in the two vertical planes containing the major and minor axes of the ellipses outside. One can check from these expressions that w_1 is continuous across the vortex edge ($|\zeta|=1$). The divergent part of order-one horizontal velocity field can be obtained from (19b). However, we do not present the corresponding cumbersome expressions. Nevertheless, note that due to the smoothing effect of the inversed Laplacian, the velocity field $\boldsymbol{\nabla}\phi_1$ obtained from injecting (20) into (19b) is continuous. The other first-order velocity corrections come from ψ_1. The equation for ψ_1 is obtained using the fact that the first-order term in (6) is zero:

$$\Delta_H \psi_1 = -\xi_{0z}\Delta_H\psi_0 + \xi_{0x}\psi_{0zx} + \xi_{0y}\psi_{0zy} - \mathcal{J}(\phi_{0z}, \xi_0). \tag{21}$$

The corresponding velocity is also continuous due to inversion of the Laplacian. Hence, the complete velocity corrections at order 1 are continuous and, in principle, calculable.

The behavior of the 3-D Kirchhoff vortex appears here to be different in several ways from the behavior of its SW analog obtained in Ref. 28: first, the equation for ψ_1 (ψ_2 in Ref. 28) will not be the same because the expressions for PV are different [compare Eq. (21) with Eq. (36) (setting $f=0$) in Ref. 28]. Second, due to the vertical differentiations needed to obtain the equation for ϕ_1, the form of the forcing for $\Delta_H\phi_1$ in the 3-D case differs significantly from the SW case. In particular, in the nonrotating SW case only expressions of the form $\zeta^n\bar{\zeta}^m$ appear on the right-hand side of equations for $\Delta\phi_2$ (our ϕ_1). In the stratified 3-D case, on the contrary, we can see from (20b) that rational fractions with poles other than zero appear making integration much more involved. The reasoning of Ref. 28, therefore, cannot be directly transposed and applied in our situation. While the corrections in question were taken into account in Ref. 28 by adding a term $\mu_3\zeta^{-3}$ to the mapping (9) and some small $[\mathcal{O}(F^2)]$ corrections to Γ_0 and ν_0, this is not sufficient here: an infinite series should be added to (9). Hence, the behavior of the 3-D vortex in each horizontal plane will be the same as the 2-D shallow water Kirchhoff vortex only at the leading order. Unfortunately, the mathematics in the following orders become too complicated to determine an explicit form of corrections.

E. Circulation, energy, and angular momentum

In this section, quantities that we will need below for the description of the long-term evolution of the vortex are calculated.

1. Circulation

Within the framework of equations (1a)–(1d) the Kelvin's circulation theorem applied to a contour $\mathcal{L}$ states:

$$\frac{d\mathcal{C}}{dt} = \oint_{\mathcal{L}} d\mathbf{l}\cdot\xi\mathbf{e}_z , \tag{22a}$$

$$= \int\int_{\mathcal{S}_\mathcal{L}} \mathbf{ds}\cdot(\xi_y\mathbf{e}_x - \xi_x\mathbf{e}_y), \tag{22b}$$

where $\mathcal{C} = \oint_{\mathcal{L}} d\mathbf{l}\cdot\mathbf{u}$ is the circulation and $\mathcal{S}_\mathcal{L}$ is a surface bounded by the contour $\mathcal{L}$.

We chose $\mathcal{L}$ to be a horizontal ellipse on the vortex edge. As ξ_0 is a function only of z inside the vortex [cf. (18a)], we see from (22b) that the first nonvanishing contribution will come from ξ_1, and hence will be $\mathcal{O}(F^2)$. Now, as $w_0 = 0$ everywhere and $w_1 = 0$ on the vortex edge [cf. (19a)], the vertical displacements of the contour, which are necessary for $d\mathbf{l}\cdot\mathbf{e}_z$ to be nonzero in (22a), will be $\mathcal{O}(F^4)$. Hence, the circulation cannot vary on times shorter than $T_3 = F^{-6}T_0$:

$$\frac{d\mathcal{C}}{dt} = \mathcal{O}(F^6). \tag{23}$$

Calculating the circulation, the following adiabatic invariant is obtained:

$$\kappa(z) = [\Gamma^2(z) - \nu^2(z)] = 2\omega\Gamma_0^2[\gamma(z)]^2 = 2\kappa_0[\gamma(z)]^2, \tag{24}$$

where $\kappa_0 = \omega\Gamma_0^2$. As (24) does not change on times shorter than T_3 for each z and given the integral constraint (14) on $\gamma(z)$, both κ_0 and $\gamma(z)$ will be considered invariant on times shorter than T_3.

2. Energy

In order to calculate the backreaction of the wave radiation, we need expressions for the leading-order energy and angular momentum. The equation of energy conservation follows from (1a)–(1d):

$$\partial_t\left(\rho_0\frac{\mathbf{u}^2}{2}+\frac{\xi^2}{2N^2}\right)+\boldsymbol{\nabla}\cdot\left[\left(\rho_0\frac{\mathbf{u}^2}{2}+\frac{\xi^2}{2N^2}\right)\mathbf{u}+P\mathbf{u}\right]=0. \quad (25)$$

At the leading order in Froude number, the energy is given by the horizontal kinetic energy. The energy of the full 3-D vortex may be calculated by vertical integration of the 2-D results.

In each plane, we integrate the energy density in a disk of radius Λ (a cutoff length) around a Kirchhoff vortex with major and minor axes $\Gamma\pm\nu$, respectively. We, thus, obtain the energy $E_{2\text{-D}}$ of the 2-D vortex (cf. Ref. 26):

$$E_{2\text{-D}}=\pi\omega^2\Gamma^4\left(\frac{1}{4}+\log\frac{\Lambda}{\Gamma}\right)=\pi\kappa^2\left(\frac{1}{4}+\log\frac{\Lambda}{\Gamma}\right). \quad (26)$$

This expression is then integrated in z using (14), and gives the energy of the 3-D vortex $E_{3\text{-D}}$:

$$E_{3\text{-D}}=\pi\kappa_0^2\left[\left(\log\frac{\Lambda}{\Gamma_0}+\frac{1}{4}\right)\mathcal{M}_4-\int_{-\infty}^{\infty}ds\,\gamma(s)^4\log\gamma(z)\right], \quad (27)$$

where

$$\mathcal{M}_4=\int_{-\infty}^{\infty}ds\,\gamma(s)^4. \quad (28)$$

For vortices of the same volume, $\mathcal{M}_4$, "flatness," increases for flatter vortices.

3. Angular momentum

The angular momentum is calculated by integrating the azimuthal velocity (u_θ in cylindrical coordinates) times radius. As for energy, we proceed by calculating the angular momentum in each horizontal plane, following Ref. 26, and then integrate in z. The 2-D calculation yields

$$M_{2\text{-D}}=\pi\omega\Gamma^2\left(\Lambda^2-\frac{\Gamma^2}{2}-\frac{\nu^2}{2}\right). \quad (29)$$

The result for the 3-D vortex is

$$M_{3\text{-D}}=\pi\kappa_0\left[-\left(\frac{\Gamma_0^2}{2}+\frac{\nu_0^2}{2}\right)\mathcal{M}_4+\Lambda^2\right]. \quad (30)$$

These expressions will be used below for calculating the backreaction of the wave emission on the vortex.

F. Pressure fluctuations far from the vortex

In order to determine the wave field emitted by the vortex, we need to calculate the farfield pressure fluctuations. It is necessary first to invert the expression for χ when $\chi\gg1$ (or equivalently $\zeta\gg1$). The inversion of (9) yields

$$\zeta=\frac{\chi}{\Gamma_0}+\mathcal{O}(\chi^{-1}). \quad (31)$$

This expression for ζ is then injected into the expression for pressure (17a):

$$P_0^{(e)}=\frac{1}{2}\omega^2\Gamma_0^4\gamma^2(z)\left(-\frac{1}{r^2}+\frac{\nu_0}{\Gamma_0 r^2}\cos(2\theta-\omega t)\right)+\mathcal{O}(r^{-3}), \quad (32)$$

where $\chi=re^{i\theta}$. The first term in this formula is monopolar and static. The second term is quadrupolar and oscillating in time and will be matched with the wave field.

III. THE FARFIELD

A. Scaling in the outer (wave) region

The scaling that we have used to obtain Eqs. (5a)–(5e) does not work anymore at large distances from the vortex. There, the fields vary at a scale greater than L and the velocity will be weaker. The order of the nonlinear terms, therefore, need to be reevaluated.

The equations are rescaled using $F^{-1}L$ as a horizontal length scale, and H as a vertical length scale. The space coordinates scaled with λ will be denoted by capital letters (X, Y, or R). The velocity far from the region where the potential vorticity is nonzero decays as $1/r$; at distances that scale as L/F, the horizontal velocity therefore scales as FU, and the vertical velocity as $W=F^2UH/L$. The time scale is the same as in the inner region, that is L/U.

With this scaling the EB equations (1a)–(1d) yield

$$\partial_t\mathbf{u_H}+\boldsymbol{\nabla}P+F^2\mathbf{u}\cdot\boldsymbol{\nabla}\mathbf{u_H}=0, \quad (33a)$$

$$\partial_z P-\xi+F^4(\partial_t w+F^2\mathbf{u}\cdot\boldsymbol{\nabla}w)=0, \quad (33b)$$

$$\partial_t\xi+w+F^2\mathbf{u}\cdot\boldsymbol{\nabla}\xi=0, \quad (33c)$$

$$\partial_X u+\partial_Y v+\partial_z w=0. \quad (33d)$$

Because of the special form of the leading-order velocity field (axisymmetric and purely azimuthal), the zeroth-order advective terms are zero. Hence, linear gravity waves are both order 0 and order 1 solutions.

B. The matching procedure

First, we note that, due to the different scalings in the inner and outer region ($R=rF$ and $u\sim FU$ in the outer region), the terms with r^{-2} in $P_0^{(e)}$ [cf. (32)] will match with the first-order term $P_1^{(w)}$ in the wave region.

In the Appendix, we display the general form of the wave fields in cylindrical coordinates. Retaining only symmetric in z terms, this general form is

$$P_1^{(w)}(R,\theta,z,t)=\sum_n a_n\int_0^\infty du\,\hat{\mathcal{F}}_n^s(u)\cos(uz)\times H_n^{(2)}(Ru\nu)e^{i(n\theta-\nu t)}, \quad (34)$$

where $H_n^{(2)}$ is the Hankel function.

Requiring the farfield fluctuations of the pressure obtained in (32) to be equal to the near-field fluctuations of the wave field imposes $n=2$ and $\nu=\omega$, thus reducing the general form of the wave field to

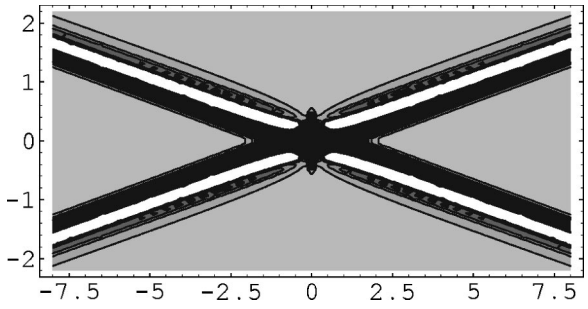

FIG. 2. Vertical cross section of the pressure perturbations corresponding to waves given by expression (37a). The pattern is very similar to the "cross" observed around an oscillating cylinder in a stratified fluid.

$$P_1^{(w)}(R,\theta,z,t)=Ae^{i\delta}\int_0^\infty du\hat{\mathcal{F}}^s(u)\cos(uz)\times H_2^{(2)}(Ru\omega)e^{i(2\theta-\omega t)}, \tag{35}$$

where A is a real and positive amplitude, and δ is a phase.

To obtain the near-field wave asymptotics, we use the following asymptotics of the Hankel function:[32]

$$H_n^{(2)}(\chi)\sim\frac{i}{\pi}\Gamma(n)\left(\frac{\chi}{2}\right)^{-n}. \tag{36}$$

Matching of the fluctuating part of $P_0^{(e)}$ and the real part of $P_1^{(w)}$ gives for $\hat{\mathcal{F}}^s(u)$, A and δ:

$$\hat{\mathcal{F}}^s(u)=2\pi u^2\int_0^{+\infty}ds[\gamma(s)]^2\cos(us), \tag{37a}$$

$$A=\frac{\pi\omega^4\Gamma_0^3\nu_0}{8}=\frac{\pi\kappa_0^4\nu_0}{8\Gamma^5},\quad \delta=-\frac{\pi}{2}. \tag{37b}$$

The emitted waves are of order F^2 in the outer region and are, thus, rather weak.

C. Description of the emitted wave field

In the first approximation, as vortex dimensions are much smaller than the characteristic wavelength, the waves can be considered as emitted from a point source. Waves are excited at a single frequency and we therefore expect, from the dispersion relation and the expression of the group velocity, that they will propagate along a cone (cf. Ref. 14). A plot of the intensity of the perturbation in a vertical plane (Fig. 2) shows that the situation is indeed close to this. Their wave vectors being of order $(1/\lambda,1/H)$, the energy will propagate at a small angle of order $FH/L=F^2$ to the horizontal. Furthermore, as waves propagate in a layer of constant thickness along the cone, their amplitude decreases as $1/\sqrt{r}$ in the radial direction.

However, the source is not exactly a point source, but rather an annular region where the fluctuations due to the vortex motion occur at a horizontal length scale λ. Thus, qualitatively, the rays of propagation of the emitted waves form a hyperboloid that deviates from the asymptotic cone, but only in the vicinity of the origin. The difference is not visible in Fig. 2, but becomes apparent in Fig. 3(a), where the phase lines on the surface of the cone have been plotted. These lines can be interpreted as approximate rays, indicating the origin of the waves, which shows that their propagation is not exactly radial from the source.

The intensity of the perturbations in the horizontal plane above or below the vortex is plotted in Fig. 3(b), and has a form of a fraction of a spiral (which is natural for waves propagating at a constant speed away from a rotating source, just like water from a rotating hose). As the waves propagate along a cone, the spiral wraps the cone.

D. Fluxes of energy and angular momentum associated with the wave field

The fluxes of energy and angular momentum will be calculated for the wave field of the form

$$P_1(R,\theta,z,t)=A\int_0^{+\infty}du\hat{\mathcal{F}}^s(u)\cos(uz)\times H_2^{(2)}(Ru\omega)e^{i(2\theta-\omega t+\delta)}. \tag{38}$$

The energy flux at the leading order in the exterior region is

$$\mathbf{f}_e=P_1\mathbf{u}_1. \tag{39}$$

The total flux of energy will be obtained by integrating this expression over a cylindrical surface surrounding the vortex. As the amplitude of the wave field decays fast in the vertical direction, we do not need to consider the energy flux through the top and the bottom parts of the cylinder. Only u_{1R} is, thus, needed; it can be obtained using Eq. (33a) at the first order in cylindrical coordinates:

$$\partial_t u_{1R}=-\partial_R P_1, \tag{40}$$

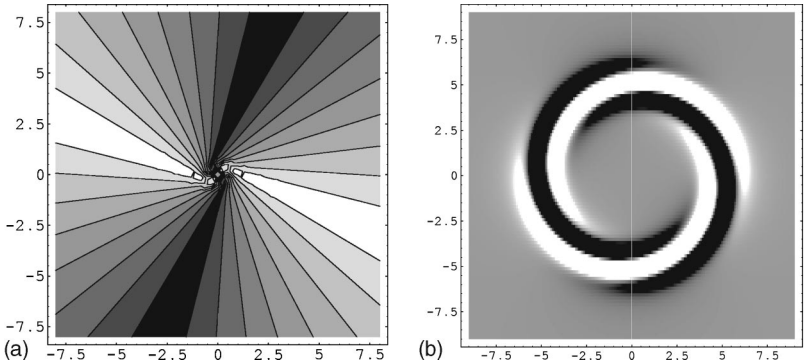

FIG. 3. (a) Phase lines plotted on the cone with angle to the horizontal equal to the angle at which the energy of the waves propagate (F^2). The region of wave generation appears as a ring at a certain distance from the center, i.e., from the vortex. Note that this plot is obtained from the farfield expressions, so the very center part of the figure is not representative. (b) Pressure perturbation due to the waves in a horizontal plane above the vortex; vortex thickness is 0.2, $\omega=0.2$, and the level of the horizontal plane is $z=1$.

which yields

$$u_{1R}=A\int_0^\infty du\hat{\mathcal{F}}^s(u)\cos(uz)u \times[J_2'(uR\omega)\sin(2\theta-\omega t+\delta) -Y_2'(uR\omega)\cos(2\theta-\omega t+\delta)]. \quad (41)$$

The total flux of energy across the cylindrical surface of radius R is

$$F_E=A^2\int_{-\infty}^{+\infty}dz\int_0^{2\pi}Rd\theta\int_0^\infty du\int_0^\infty du'\hat{\mathcal{F}}^s(u)\hat{\mathcal{F}}^s(u')u' \times\cos(uz)\cos(u'z)[\sin^2 J_2'Y_2-\cos^2 J_2Y_2' +\cos\sin(J_2J_2'-Y_2Y_2')], \quad (42)$$

where the arguments $(uR\omega)$, $(u'R\omega)$, and $(2\theta-\omega t)$ of the Bessel and trigonometric functions have been omitted for brevity. Carrying out integrations in z and θ, and using the known property of the Wronskian of the Bessel functions,[32]

$$J_n'(a)Y_n(a)-J_n(a)Y_n'(a)=\frac{2}{\pi a}, \quad (43)$$

the total energy flux is obtained:

$$F_E=\frac{A^2}{\omega}\int_0^{+\infty}du[\hat{\mathcal{F}}^s(u)]^2. \quad (44)$$

The angular momentum flux will be calculated in a similar way. The equation for the vertical component of the angular momentum, derived from the EB equations, is

$$\frac{\partial m_3}{\partial t}+\nabla[m_3\mathbf{u}+P(\mathbf{e}_z\times\mathbf{R})]=0, \quad (45)$$

where $m_3=Ru_\theta$ is the vertical component of the angular momentum. The linear term of $\mathbf{f}_m=m_3\mathbf{u}+P(\mathbf{e}_z\times\mathbf{R})$ will yield zero when integrated over an infinite vertical surface because of periodicity of P_1 in θ. As only one term remains, scaling considerations are unnecessary and calculations similar to the previous ones give

$$F_M=\frac{2A^2}{\omega^2}\int_0^\infty du[\hat{\mathcal{F}}^s(u)]^2. \quad (46)$$

Note that the energy flux and the angular momentum flux are simply related: $F_M=(2/\omega)F_E$.

IV. THE BACKREACTION OF THE RADIATION

The evolution of the vortex due to the loss of energy and angular momentum by radiation is supposed to be adiabatic, i.e., attributed to a slow change of its parameters. From (27) and (30), we get

$$\frac{dE_{3\text{-D}}}{dt}=-\pi\kappa_0^2\mathcal{M}_4\frac{1}{\Gamma_0}\frac{d\Gamma_0}{dt}, \quad (47a)$$

$$\frac{dM_{3\text{-D}}}{dt}=-\pi\kappa_0\mathcal{M}_4\left(\Gamma_0\frac{d\Gamma_0}{dt}+\nu_0\frac{d\nu_0}{dt}\right). \quad (47b)$$

Using (37b), (44), and (46), and noting that the waves' amplitudes are $\mathcal{O}(F^2)$, we have

$$F_E=F^4\frac{\pi^2\kappa_0^7G}{64}\frac{\nu_0^2}{\Gamma_0^8}, \quad (48a)$$

$$F_M=F^4\frac{2\pi^2\kappa_0^6G}{64}\frac{\nu_0^2}{\Gamma_0^6}, \quad (48b)$$

where $G=\int_{-\infty}^\infty[\hat{\mathcal{F}}^s(u)]^2du$. With the help of the energy and angular momentum conservation laws the following coupled evolution equations are obtained:

$$\frac{d}{dt_2}(\Gamma_0^2)=\frac{d}{dt_2}(\nu_0^2)=\frac{\pi G\kappa_0^5}{32\mathcal{M}_4}\frac{\nu_0^2}{\Gamma_0^6}, \quad (49)$$

where $t_2=F^4t_0$ is adequately rescaled time. The conservation of the area of the ellipse in each horizontal plane readily follows from (49) by integration:

$$\Gamma_0^2-\nu_0^2=S=\text{const}, \quad (50)$$

and, hence, the total volume of the vortex is conserved. Denoting $y=\nu_0^2$ and integrating (49), we obtain

$$\int_{\nu_{0i}^2}^{\nu_0^2}dy\frac{(S+y)^3}{y}=\frac{\pi G\kappa_0^5}{32\mathcal{M}_4}t_2. \quad (51)$$

These results reproduce the ones of Ref. 26. (A correction, however, has to be made to Eq. (16) of Ref. 26, which parallels Eq. (51) here. Indeed, the dependence on ω of the coefficient A_0 was neglected there; the full equation (16) reads as $\int_{|\beta_0|^2}^{|\beta|^2}(dy/y)(S+Ny)^{N+2}=N^{2N+3}\Gamma^{2N+3}/\{(2c)^{2N+2}[(N+1)!]^2(2\pi)^{2N+2}\}[(N+1)/2]^{N+1}t$.)

Similarly, we obtain for Γ_0,

$$\int_{\Gamma_{0i}^2}^{\Gamma_0^2}dx\frac{x^3}{x-S}=\frac{\pi G\kappa_0^5}{32\mathcal{M}_4}t_2. \quad (52)$$

The integrands in the last two equations are rational fractions and can be easily integrated:

$$\frac{1}{3}\left[\left(\frac{\Gamma_0}{\Gamma_{0i}}\right)^6-1\right]+\frac{S}{2\Gamma_{0i}^2}\left[\left(\frac{\Gamma_0}{\Gamma_{0i}}\right)^4-1\right]+\frac{S^2}{\Gamma_{0i}^4}\left[\left(\frac{\Gamma_0}{\Gamma_{0i}}\right)^2-1\right] +\frac{S^3}{\Gamma_{0i}^6}\log\left(\frac{\Gamma_0^2-S}{\Gamma_{0i}^2-S}\right)=\frac{\pi G\kappa_0^5}{32\mathcal{M}_4\Gamma_{0i}^6}t_2, \quad (53a)$$

$$\frac{1}{3}\left[\left(\frac{\nu_0}{\nu_{0i}}\right)^6-1\right]+\frac{3S}{2\nu_{0i}^2}\left[\left(\frac{\nu_0}{\nu_{0i}}\right)^4-1\right]+\frac{3S^2}{\nu_{0i}^4}\left[\left(\frac{\nu_0}{\nu_{0i}}\right)^2-1\right] +\frac{2S^3}{\nu_{0i}^6}\log\left(\frac{\nu_0}{\nu_{0i}}\right)=\frac{\pi G\kappa_0^5}{32\mathcal{M}_4\nu_{0i}^6}t_2, \quad (53b)$$

where the index i corresponds to initial values.

As an example, we consider a vortex that is initially slightly nonaxisymmetric with $\Gamma_0=1$ and $\nu_0=0.01$. It can be seen from (49) or from (53b) (in which the dominant term is the one preceded by $2S^3/\nu_{0i}^6$) that ν_0 is then expected to grow exponentially for initial times (cf. Fig. 4):

$$\nu_0\sim\nu_{0i}e^{(\pi G\kappa_0^5/64\mathcal{M}_4\Gamma_{0i}^6)t_2}. \quad (54)$$

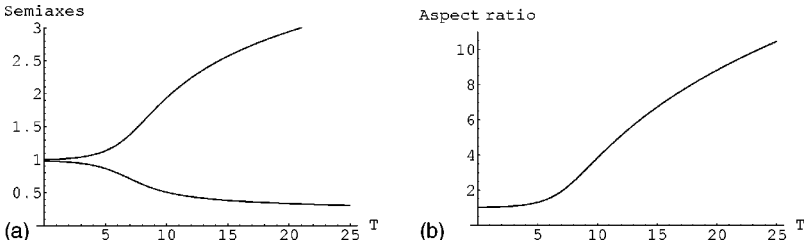

FIG. 4. (a) Evolution of the semiaxes $\Gamma \pm \nu$ at height $z=0$ of a 3-D Kirchhoff vortex. Initial values are 1 and 0.98. Time units are scaled as $T_2 = T_0/F^4$. At initial times, the evolution is exponential. For longer times, the time law takes the same form as the law obtained for point vortices [cf. Eq. (55)], but we then reach values for the aspect ratio that are not realistic. (b) Evolution of the aspect ratio of the same vortex.

As the semiaxes of the elliptic horizontal cross section are related to ν via $\Gamma \pm \nu$, an elongation of the vortex at initial times results. As the vortex elongates, the rate of rotation decreases [cf. (24)]. [Note that, unlike Ref. 28, here we do not have a frequency threshold for the wave emission (f in SW)—this is a difference between rotating and nonrotating fluid.]

The time scale of thus obtained growth is very slow, for it scales as $F^{-4}L/U$. If elongation continues for longer times, we would have $(\Gamma_0/\Gamma_{0i}) \gg 1$ and $(\nu_0/\nu_{0i}) \gg 1$ and the first terms in both equations (53) become dominant. An elongation law of the same form as that for the distance between two point vortices of equal intensity (cf. Ref. 25) then follows for late stages of evolution:

$$\Gamma_0 = \Gamma_{0i}(1 + t_2/\tau)^{1/6}, \tag{55}$$

where $\tau = (32\mathcal{M}_4\Gamma_{0i}^6)/(3\pi G \kappa_0^5)$. In this form, however, it is valid only for large aspect ratios of the ellipses (see Fig. 4) and, as discussed below, the vortex is likely to become unstable before that.

V. SUMMARY AND DISCUSSION

In the present paper we addressed the question of IGW emission from an isolated pancake vortex of the kind observed in laboratory experiments and numerical simulations of strongly stratified flows. There are two stages of wave production by perturbations bearing vorticity in stratified flows. The first stage corresponds to the adjustment of arbitrary localized disturbances to the (balanced) state of hydrostatic and cyclostrophic equilibrium that is accompanied by emission of the ''redundant'' part in the form of outgoing waves. This is, thus, a transient wave emission. The linear treatment of this process is presented in Ref. 17 and may be pursued further on perturbatively in Froude number, following the lines of Ref. 33, where the geostrophic adjustment was studied. The second stage corresponds to a permanent Lighthill radiation by the *balanced* but nonstationary vortex motions, and it was this latter process we were concentrated on in the present paper. We, thus, treated the problem as a radiation one. Any radiation problem requires exact knowledge of the wave source, and for this purpose we constructed an explicit example of a rotating ellipsoidal region of constant PV in cyclostrophic balance, obeying the EB equations at the leading order in the Froude number. In doing this we essentially used the quasibidimensionalization of stratified fluids due to a strong stratification, which allowed us to use the classical 2-D Kirchoff vortex as the base for our construction. The explicit knowledge of the vortex field allowed us to calculate analytically the emitted wave field and to derive the effects of the backreaction of the wave radiation. The backreaction's calculation shows that the IGW emission leads to very slow but systematic changes in the vortex shape.

Some remarks are in order in what concerns the backreaction, however. First, the elongation scenario discussed in the previous section is valid under the hypothesis that there are no other factors inducing slow evolution of the vortex at time scales T_2 or faster (say, at the time scale $T_1 = F^{-2}T_0$). This latter may be necessary, for instance, if resonances arise while calculating the higher-order corrections to the (vortical) near-field (without any reference to the far wave field) that have to be killed by slow time dependence of lower-order fields. Due to their excessive (and rapidly increasing with the order of the perturbation theory) technical complexity we did not undertake here the corresponding calculations and, hence, cannot guarantee the validity of the above-mentioned hypothesis. One remark here is that, the Kirchoff vortex being an exact solution of the 2-D Euler equations, such evolution could come uniquely from the 3-D effects and, therefore, would mean that the widely believed scenario of bidimensionalization of strongly stratified flows is broken already in the next-to-leading order in stratification (cf. the discussion at the end of Sec. II F). Albeit unplausible, we do not see at present how such evolution could be *a priori* excluded. This question deserves a further investigation.

Second, even if the elongation due to the backreaction of the wave radiation is not accompanied by other slow motions, it is intuitively clear that it cannot last and should end up with some sort of instability. Unfortunately, nothing is known on stability of the ellipsoidal regions of PV in the stratified fluid. Again, the corresponding analytical calculations are very complex. Stability calculations do exist for similar ellipsoidal vortices in a much simpler context of quasigeostrophic dynamics,[30] but modes of instability may, of course, differ significantly in the two cases. The 2-D Kirchhoff vortex is known[34] to be unstable when its aspect ratio exceeds 3. It is unlikely that 3-D effects may prevent this 2-D instability so we anticipate that at least for aspect ratios greater than 3 the pancake vortex will be destabilized. If, because of imposed reflectional symmetry, as in Ref. 28, the first instability mode cannot be excited, the aspect ratio might grow further. In two dimensions, as argued in Ref. 28, the wave resonances excite a quadrupolar (mode 4) instability of the elliptic vortex for aspect ratios beyond ~4.6, corresponding to $(\nu/\Gamma)^2 = \sqrt{2} - 1$. Whether the same is true for 3-D stratified vortices remains an open question. In any case, it is clear that once elongated enough the vortex is prone to instabilities and, hence, although slow, the backreaction of

the wave radiation will alter vortex dynamics in the 3-D stratified fluid, as it was the case in 2-D acoustics and shallow water. This indicates that a strict slow manifold of purely vortex motions does not exist in stratified nonrotating fluids and sets a time limit ($\sim F^{-4}$) for a reliable description of slow motions by filtering IGW.

ACKNOWLEDGMENT

R.P. acknowledges support from ACI ''jeunes chercheurs'' (CNRS) No. 0693.

APPENDIX: INTERNAL GRAVITY WAVES IN CYLINDRICAL COORDINATES

We recall the wave equation one can obtain from the equations of motion as they are scaled for the outer region (33a)–(33d):

$$\partial_{zz}\partial_{tt}w+\Delta_H w=0. \tag{A1}$$

We separate variables and look for solutions w of the form

$$w(R,z,\theta,t)=g(R)e^{i(n\theta-\nu t)}h(z), \tag{A2}$$

where $h(z)$ is of the form e^{imz}, and g verifies the following equation:

$$\frac{d^2g}{dR^2}+\frac{1}{R}\frac{dg}{dR}+\left(m^2\nu^2-\frac{n^2}{R^2}\right)g=0. \tag{A3}$$

Using the change of variables $\rho=m\nu R$, one gets the canonical Bessel equation:

$$\frac{d^2g}{d\rho^2}+\frac{1}{\rho}\frac{dg}{d\rho}+\left(1-\frac{n^2}{\rho^2}\right)g=0. \tag{A4}$$

Solutions corresponding to the radiation boundary condition at infinity are Hankel functions of the second kind. We then reconstruct the complete solution:

$$w(R,\theta,z,t)=\sum_n a_n\int_0^\infty du[\hat{\mathcal{F}}_n^s(u)\cos(uz)+\hat{\mathcal{F}}_n^a(u)\sin(uz)]H_n^{(2)}(Ru\nu)e^{i(n\theta-\nu t)}. \tag{A5}$$

The same equation as (A1) can be obtained for the pressure. Its expression will therefore be of the same form as (A5).

If the vertical profile of the vortex is symmetric in z, only the functions $\hat{\mathcal{F}}_n^s(u)$ need to be considered: this is the expression used for the matching.

[1]J. J. Riley, R. W. Metcalfe, and M. A. Weissman, ''Direct numerical simulations of homogeneous turbulence in density stratified fluids,'' in *Proceedings of the AIP Conference on Nonlinear Properties of Internal Waves* (AIP, Woodbury, 1981), pp. 79–112.
[2]D. K. Lilly, ''Stratified turbulence and the mesoscale variability of the atmosphere,'' J. Atmos. Sci. **40**, 749 (1983).
[3]J. J. Riley and M.-P. Lelong, ''Fluid motions in the presence of strong stable stratification,'' Annu. Rev. Fluid Mech. **32**, 613 (2000).
[4]O. Métais and J. R. Herring, ''Numerical simulations of freely evolving turbulence in stably stratified fluids,'' J. Fluid Mech. **202**, 117 (1989).
[5]G. R. Spedding, F. K. Browand, and A. M. Fincham, ''The long-time evolution of the initially turbulent wake of a sphere in a stable stratification,'' Dyn. Atmos. Oceans **23**, 171 (1996).
[6]M. Bonnier, O. Eiff, and P. Bonneton, ''On the density structure of far-wake vortices in a stratified fluid,'' Dyn. Atmos. Oceans **31**, 117 (2000).
[7]A. M. Fincham, T. Maxworthy, and G. R. Spedding, ''Energy dissipation and vortex structure in freely decaying, stratified grid turbulence,'' Dyn. Atmos. Oceans **23**, 155 (1996).
[8]G. R. Spedding, F. K. Browand, and A. M. Fincham, ''Turbulence, similarity scaling and vortex geometry in the wake of a towed sphere in a stably stratified fluid,'' J. Fluid Mech. **314**, 53 (1996).
[9]A. J. Majda and M. J. Grote, ''Model dynamics and vertical collapse in decaying strongly stratified flows,'' Phys. Fluids **9**, 2932 (1997).
[10]P. Billant and J. M. Chomaz, ''Experimental evidence for a new instability of a vertical columnar vortex pair in a strongly stratified fluid,'' J. Fluid Mech. **418**, 167 (2000).
[11]P. Billant and J. M. Chomaz, ''Theoretical analysis of the zigzag instability of a columnar vortex pair in a strongly stratified fluid,'' J. Fluid Mech. **419**, 29 (2000).
[12]J. B. Flor and G. J. F. van Heijst, ''Stable and unstable monopolar vortices in a stratified fluid,'' J. Fluid Mech. **311**, 257 (1996).
[13]M. Beckers, R. Verzicco, H. J. H. Clercx, and G. J. F. Van Heist, ''Dynamics of pancake-like vortices in a stratified fluid: experiments, theory and numerical simulations,'' J. Fluid Mech. **433**, 1 (2001).
[14]J. M. Lighthill, *Waves in Fluids* (Cambridge University Press, Cambridge, 1978).
[15]P. Bonneton, J. M. Chomaz, and E. J. Hopfinger, ''Internal waves produced by the turbulent wake of a sphere moving horizontally in a stratified fluid,'' J. Fluid Mech. **254**, 23 (1993).
[16]P. Bonneton, J. M. Chomaz, E. J. Hopfinger, and M. Perrier, ''The structure of the turbulent wake and the random internal wave field generated by a moving sphere in a stratified fluid,'' Dyn. Atmos. Oceans **23**, 299 (1996).
[17]J. M. Lighthill, ''Internal waves and related initial-value problems,'' Dyn. Atmos. Oceans **23**, 3 (1996).
[18]P. Caillol and V. Zeitlin, ''Kinetic equations and stationary energy spectra of weakly nonlinear internal gravity waves,'' Dyn. Atmos. Oceans **32**, 81 (2000).
[19]R. Ford, M. E. McIntyre, and W. A. Norton, ''Balance and the slow quasi-manifold: some explicit results,'' J. Atmos. Sci. **57**, 1236 (2000).
[20]J. M. Lighthill, ''On sound generated aerodynamically. I. General theory,'' Proc. R. Soc. London, Ser. A **211**, 564 (1952).
[21]S. C. Crow, ''Aerodynamic sound emission as a singular perturbation problem,'' Stud. Appl. Math. **49**, 21 (1970).
[22]D. G. Crighton, ''Acoustics as a branch of fluid mechanics,'' J. Fluid Mech. **106**, 261 (1981).
[23]T. Kambe, ''Acoustic emissions by vortex motions,'' J. Fluid Mech. **173**, 643 (1986).
[24]V. I. Klyatskin, ''Emission of sound by a system of vortices,'' Izv. Akad. Nauk SSSR, Mekh. Zhidk. Gaza **6**, 87 (1966) (in Russian).
[25]V. M. Gryanik, ''Emission of sound by linear vortical filaments,'' Izv. Atmos. Ocean. Phys. **19**, 150 (1983).
[26]V. Zeitlin, ''On the backreaction of acoustic radiation for distributed two-dimensional vortex structures,'' Phys. Fluids A **3**, 1677 (1991).
[27]H. Lamb, *Hydrodynamics*, 6th ed. (Dovers, New York, 1932).
[28]R. Ford, ''The response of a rotating ellipse of uniform potential vorticity to gravity wave radiation,'' Phys. Fluids **6**, 3694 (1994).
[29]B. Legras and V. Zeitlin, ''Conformal dynamics for vortex motions,'' Phys. Lett. A **167**, 265 (1992).
[30]S. P. Meacham, ''Quasigeostrophic, ellipsoidal vortices in a stratified fluid,'' Dyn. Atmos. Oceans **16**, 189 (1992).
[31]H. Hashimoto, T. Shimonishi, and T. Miyazaki, ''Quasigeostrophic ellipsoidal vortices in a two-dimensional strain-field,'' J. Phys. Soc. Jpn. **68**, 3863 (1999).
[32]M. Abramowitz and I. Stegun, *Handbook of Mathematical Functions*, National Bureau of Standards, Applied Mathematics Series, 1964.
[33]G. M. Reznik, V. Zeitlin, and M. Ben Jelloul, ''Nonlinear theory of the geostrophic adjustment. Part 1. Rotating shallow water model,'' J. Fluid Mech. **445**, 93 (2001).
[34]A. E. H. Love, ''On the stability of certain vortex motions,'' Proc. London Math. Soc. **25**, 18 (1893).